Vibro-Acoustic Simulation of Automotive Piping and Exhaust Systems

Lothar Gaul[1], Jan Herrmann, Michael Junge

Institut for Nonlinear Mechanics, Research Group Prof. Gaul, University of Stuttgart, 70569 Stuttgart,
[1] *E-Mail:gaul@inm.uni-stuttgart.de*

Einleitung

The influence of the acoustic field on the structural dynamics is a common issue in automotive applications. An example is the pressure-induced structure-borne sound of piping and exhaust systems. Efficient model order reduction and substructuring techniques accelerate the finite element analysis and enable the vibro-acoustic optimization of such complex systems with acoustic fluid-structure interaction. This research reviews the application of the Craig-Bampton and Rubin method to fluid-structure coupled systems and presents two automotive applications. First, a fluid-filled brake-pipe system is assembled by substructures or superelements according to the Craig-Bampton method. Fluid and structural partitions are fully coupled in order to capture the interaction between the pipe shell and the heavy fluid inside the pipe. Second, a rear muffler with an air-borne excitation is analyzed. Here, the Rubin and the Craig-Bampton method are used to separately compute the uncoupled component modes of both the acoustic and structural domain. These modes are then used to compute a reduced model which incorporates full acoustic-structure coupling. For both applications, transfer functions are computed and compared to the results of dynamic measurements.

Introduction

Elastic piping and exhaust systems are often characterized by (hydro-)acoustic sources. An example for a hydroacoustic excitation in hydraulic pipes such as fuel and brake-pipes is the operation of pumps and valves which leads to oscillating pressure pulsations within the pipe. As a result, pressure waves propagate along the pipe and excite the pipe shell due to the heavy fluid-structure coupling [1, 2, 3]. Finally, the pressure-induced structure-borne sound is transmitted to attachment structures which leads to undesired noise and vibration levels [4]. A similar excitation scenario is found in automotive exhaust systems where the exhaust gas acts as a strong acoustic source which also leads to pressure-induced structure-borne sound and undesired sound radiation [5]. To predict the vibro-acoustic behavior of such mechanical systems, three-dimensional models including full coupling of the two-field problem are needed. It is particularly important to include bending modes of the structure, which are predominantly responsible for sound and vibration harshness. The finite element method [6] is considered as the appropriate discretization method to investigate the dynamics of the interior vibro-acoustic problem including the coupling between the inner fluid and the pipe shell. The boundary element method might be used to determine the sound radiation in the exterior field [7]. The main problem of fully discretized models are large computation times and extensive computer memory. Model order reduction and substructuring techniques such as the well-known component mode synthesis overcome this limitation. This research shows how the Craig-Bampton [8] and the Rubin method [9] are applied to efficiently compute the hydroand vibro-acoustic response of two automotive applications. First, a fluid-filled brake-pipe system is analyzed which is characterized by a heavy fluid-structure coupling between the water inside the pipe and the flexible pipe shell. The Craig-Bampton method is applied which leads to a considerable model order reduction and to moderate computation times. Moreover, the influence of a cross-section change on the hydraulic transfer function is analyzed and the results are validated by a hydraulic test bench operating in the kHz-range. Secondly, an automotive exhaust system is analyzed which is an example of light fluid-structure coupling between the exhaust gas and the structure of the expansion chamber. Here, the Rubin and the Craig-Bampton are used to separately determine the uncoupled component modes of both the acoustic and structural domain. These modes are used to compute a reduced model including full acoustic-structure coupling. Measurements are performed and the vibro-acoustic response is compared to the results of the simulation including the proposed model reduction technique.

Finite Element Based Substructure Techniques

This chapter briefly summarizes the application of the Craig-Bampton and the Rubin method on fluid-structure coupled systems. Both methods are used to reduce the order of the corresponding finite element model of each component and to assemble the overall mechanical system. The linear wave equation for a fluid at rest is used for low Mach numbers as encountered in most piping and exhaust systems [1]. The acoustic field is coupled to the structural dynamic equations at the fluid-structure interface [6], where two coupling conditions hold, namely the Euler equation and the reaction force axiom. The corresponding finite element formulation leads to coupled discretized equations in terms of nodal structural displacements u and nodal acoustic excess pressures p

$$\begin{bmatrix} \boldsymbol{M}_S & \boldsymbol{0} \\ \rho_0 \boldsymbol{C}^T & \boldsymbol{M}_a \end{bmatrix} \cdot \begin{bmatrix} \ddot{\boldsymbol{u}} \\ \ddot{\boldsymbol{p}} \end{bmatrix} + \begin{bmatrix} \boldsymbol{D}_S & \boldsymbol{0} \\ \boldsymbol{0} & \boldsymbol{D}_a \end{bmatrix} \cdot \begin{bmatrix} \dot{\boldsymbol{u}} \\ \dot{\boldsymbol{p}} \end{bmatrix} + \begin{bmatrix} \boldsymbol{K}_S & -\boldsymbol{C} \\ \boldsymbol{0} & \boldsymbol{K}_a \end{bmatrix} \cdot \begin{bmatrix} \boldsymbol{u} \\ \boldsymbol{p} \end{bmatrix} = \begin{bmatrix} \boldsymbol{f}(t) \\ \boldsymbol{q}(t) \end{bmatrix}. \tag{1}$$

In the above equation, index “s” denotes the structural partition, whereas index “a” characterizes the acoustic fluid. The discretized equations include mass matrices $\boldsymbol{M}_{\mathrm{s,a}}$, stiffness matrices $\boldsymbol{K}_{\mathrm{s,a}}$, viscous damping matrices $\boldsymbol{D}_{\mathrm{s,a}}$, as well as the coupling matrix $\boldsymbol{C}$. Forces and fluxes are given as $\boldsymbol{f}(\mathrm{t})$ and $\boldsymbol{q}(\mathrm{t})$. Hereby, the classical unsymmetric formulation with displacements and pressures as field variables is used. It is worthy of note that alternative representations use the acoustic

velocity potential as field variable [10] which leads to a symmetric formulation of Eq. (1).

Craig-Bampton Method

The adaptation of the Craig-Bampton method to mechanical systems with acoustic fluid-structure coupling has been developed in [11]. For clarity, the critical steps are briefly summarized in this section. To apply the Craig-Bampton method to the acoustic-structure coupled problem, displacement and pressure DOFs are both separated into interface DOFs with index "I" and inner (free) DOFs denoted by index "F", i.e. $\boldsymbol{u} = [\boldsymbol{u}_\mathrm{I}^\mathrm{T} \quad \boldsymbol{u}_\mathrm{F}^\mathrm{T}]^\mathrm{T}$ and $\boldsymbol{p} = [\boldsymbol{p}_\mathrm{I}^\mathrm{T} \quad \boldsymbol{p}_\mathrm{F}^\mathrm{T}]^\mathrm{T}$, respectively. The matrices are partitioned accordingly. As explained in [8], the Craig-Bampton reduction basis consists of fixed interface modes and constraint modes. The fixed interface modes are obtained by solving the eigenvalue problem for the system with constrained interface DOFs

$$\left(\begin{bmatrix} \boldsymbol{K}_{s,FF} & -\boldsymbol{C}_{FF} \\ \boldsymbol{0} & \boldsymbol{K}_{a,FF} \end{bmatrix} - \omega_j^2 \begin{bmatrix} M_{s,FF} & \boldsymbol{0} \\ \rho_0 \boldsymbol{C}_{FF}^T & M_{a,FF} \end{bmatrix}\right) \cdot \begin{bmatrix} \hat{\boldsymbol{u}}_{j,F} \\ \hat{\boldsymbol{p}}_{j,F} \end{bmatrix} = \boldsymbol{0}. \tag{2}$$

The reduction bases $\boldsymbol{\Phi}$ are enriched by the fixed interface modes up to the m-th eigenvector or a certain frequency threshold (which is usually at least two times the maximum frequency of interest), such that $\boldsymbol{\Phi}_S = \left[\hat{u}_{1,F}, \ldots, \hat{u}_{m,F}\right]$ and $\boldsymbol{\Phi}_a = \left[\hat{p}_{1,F}, \ldots, \hat{p}_{m,F}\right]$. A modification of an iterative subspace solver is applied to compute the eigenvectors [12, 1]. The eigenspaces are mass-normalized in order to avoid ill-conditioning or numerical break-down. The constraint modes follow from a static of Guyan condensation [13]. The resulting reduction bases $\boldsymbol{\Gamma}_S$ and $\boldsymbol{\Gamma}_a$ are built according to Craig-Bampton method by discarding any coupling terms, i.e.

$$\begin{bmatrix} \boldsymbol{u}_\mathrm{I} \\ \boldsymbol{u}_\mathrm{F} \end{bmatrix} = \begin{bmatrix} \boldsymbol{I} & \boldsymbol{0} \\ -\boldsymbol{K}_{\mathrm{s,FF}}^{-1}\boldsymbol{K}_{\mathrm{s,FI}} & \boldsymbol{\Phi}_{\mathrm{s,FF}} \end{bmatrix} \begin{bmatrix} \boldsymbol{u}_\mathrm{I} \\ \boldsymbol{u}_\mathrm{d} \end{bmatrix} = \boldsymbol{\Gamma}_\mathrm{s}\, \boldsymbol{q}_\mathrm{s} \tag{3}$$

for the structural domain and

$$\begin{bmatrix} \boldsymbol{p}_\mathrm{I} \\ \boldsymbol{p}_\mathrm{F} \end{bmatrix} = \begin{bmatrix} \boldsymbol{I} & \boldsymbol{0} \\ -\boldsymbol{K}_{\mathrm{a,FF}}^{-1}\boldsymbol{K}_{\mathrm{a,FI}} & \boldsymbol{\Phi}_{\mathrm{a,FF}} \end{bmatrix} \begin{bmatrix} \boldsymbol{p}_\mathrm{I} \\ \boldsymbol{p}_\mathrm{d} \end{bmatrix} = \boldsymbol{\Gamma}_\mathrm{a}\, \boldsymbol{q}_\mathrm{a} \tag{4}$$

for the fluid domain, respectively. Hereby, index "d" denotes dominant modal coordinates as compared to neglected or truncated modal coordinates. Hence, $\boldsymbol{q}_\mathrm{s}$ and $\boldsymbol{q}_\mathrm{a}$ are the generalized coordinates of the reduced system. The overall reduction basis is assembled by

$$\begin{bmatrix} \boldsymbol{u} \\ \boldsymbol{p} \end{bmatrix} = \underbrace{\begin{bmatrix} \boldsymbol{\Gamma}_\mathrm{s} & \boldsymbol{0} \\ \boldsymbol{0} & \boldsymbol{\Gamma}_\mathrm{a} \end{bmatrix}}_{\boldsymbol{\Gamma} \in \mathbb{R}^{n \times n_\mathrm{r}}} \begin{bmatrix} \boldsymbol{q}_\mathrm{s} \\ \boldsymbol{q}_\mathrm{a} \end{bmatrix} \tag{5}$$

and reduces the coupled system in Eq. (1) to $n_\mathrm{r} << n$ DOFs

$$\begin{bmatrix} \boldsymbol{M}_\mathrm{s}^\diamond & \boldsymbol{0} \\ \rho_0\, \boldsymbol{C}^{\diamond\mathrm{T}} & \boldsymbol{M}_\mathrm{a}^\diamond \end{bmatrix} \begin{bmatrix} \ddot{\boldsymbol{q}}_\mathrm{s} \\ \ddot{\boldsymbol{q}}_\mathrm{a} \end{bmatrix} + \begin{bmatrix} \boldsymbol{K}_\mathrm{s}^\diamond & -\boldsymbol{C}^\diamond \\ \boldsymbol{0} & \boldsymbol{K}_\mathrm{a}^\diamond \end{bmatrix} \begin{bmatrix} \boldsymbol{q}_\mathrm{s} \\ \boldsymbol{q}_\mathrm{a} \end{bmatrix} = \begin{bmatrix} \boldsymbol{f}_\mathrm{s} \\ \boldsymbol{f}_\mathrm{a} \end{bmatrix} \tag{6}$$

where

$$\begin{aligned} M_\mathrm{s}^\diamond &= \boldsymbol{\Gamma}_\mathrm{s}^\mathrm{T} M_\mathrm{s} \boldsymbol{\Gamma}_\mathrm{s}, & M_\mathrm{a}^\diamond &= \boldsymbol{\Gamma}_\mathrm{a}^\mathrm{T} M_\mathrm{a} \boldsymbol{\Gamma}_\mathrm{a}, & K_\mathrm{s}^\diamond &= \boldsymbol{\Gamma}_\mathrm{s}^\mathrm{T} K_\mathrm{s} \boldsymbol{\Gamma}_\mathrm{s}, & K_\mathrm{a}^\diamond &= \boldsymbol{\Gamma}_\mathrm{a}^\mathrm{T} K_\mathrm{a} \boldsymbol{\Gamma}_\mathrm{a}, \\ C^\diamond &= \boldsymbol{\Gamma}_\mathrm{a}^\mathrm{T} C \boldsymbol{\Gamma}_\mathrm{s}, & f_\mathrm{s} &= \boldsymbol{\Gamma}_\mathrm{s}^\mathrm{T} f & f_\mathrm{a} &= \boldsymbol{\Gamma}_\mathrm{a}^\mathrm{T} q. \end{aligned} \tag{7}$$

Eq. (6) describes the superelement for the component mode synthesis. It is important to note that both structural and fluid interface DOFs are kept as physical DOFs which simplifies the component coupling procedure and which allows the integration of an impedance boundary condition in the reduced equations. The Craig-Bampton method is particularly efficient for piping systems, where the number of interface DOFs between the components is small compared to the inner DOFs and where repeating superelements occur. An additional reduction of the remaining interface DOFs leads to a further computational speedup and may be applied as explained in [3, 14, 15].

The coupling between the reduced component models is defined by single point contraints on the component interfaces. This holds for both the solid and the fluid domain, and implicit coupling conditions are established. They are used for the generation of an explicit transformation matrix Q to transform the component coordinates in coordinates of the assembled piping system [16]. This coupling procedure allows the subsequent summation of n_sub substructure contributions. An alternative way to couple the superelements using Lagrangian multipliers is shown in [17]. The global dynamic system of equations with the global reduced coordinates $\boldsymbol{q} = [\boldsymbol{q}_\mathrm{s} \ \boldsymbol{q}_\mathrm{a}]^\mathrm{T}$ is given as

$$\boldsymbol{M}_\mathrm{g}\ddot{\boldsymbol{q}} + \boldsymbol{D}_\mathrm{g}\dot{\boldsymbol{q}} + \boldsymbol{K}_\mathrm{g}\boldsymbol{q} = \boldsymbol{f}_\mathrm{g}, \tag{8}$$

whereas the system matrices $\boldsymbol{M}_\mathrm{g}$ and $\boldsymbol{K}_\mathrm{g}$ are assembled as

$$\boldsymbol{M}_\mathrm{g} = \sum_{i=1}^{n_\mathrm{sub}} \begin{bmatrix} \boldsymbol{Q}_{\mathrm{s},i}^\mathrm{T} \boldsymbol{M}_{\mathrm{s},i}^\diamond \boldsymbol{Q}_{\mathrm{s},i} & \boldsymbol{0} \\ \rho_0 \boldsymbol{Q}_{\mathrm{a},i}^\mathrm{T} \boldsymbol{C}_i^{\diamond\mathrm{T}} \boldsymbol{Q}_{\mathrm{s},i} & \boldsymbol{Q}_{\mathrm{a},i}^\mathrm{T} \boldsymbol{M}_{\mathrm{a},i}^\diamond \boldsymbol{Q}_{\mathrm{a},i} \end{bmatrix}, \tag{9}$$

$$\boldsymbol{K}_\mathrm{g} = \sum_{i=1}^{n_\mathrm{sub}} \begin{bmatrix} \boldsymbol{Q}_{\mathrm{s},i}^\mathrm{T} \boldsymbol{K}_{\mathrm{s},i}^\diamond \boldsymbol{Q}_{\mathrm{s},i} & -\boldsymbol{Q}_{\mathrm{s},i}^\mathrm{T} \boldsymbol{C}_i^\diamond \boldsymbol{Q}_{\mathrm{a},i} \\ \boldsymbol{0} & \boldsymbol{Q}_{\mathrm{a},i}^\mathrm{T} \boldsymbol{K}_{\mathrm{a},i}^\diamond \boldsymbol{Q}_{\mathrm{a},i} \end{bmatrix}. \tag{10}$$

The global damping matrix is given as

$$\boldsymbol{D}_\mathrm{g} = \sum_{i=1}^{n_\mathrm{sub}} \begin{bmatrix} \alpha_{\mathrm{s},i} \boldsymbol{Q}_{\mathrm{s},i}^\mathrm{T} \boldsymbol{M}_{\mathrm{s},i}^\diamond \boldsymbol{Q}_{\mathrm{s},i} + \beta_{\mathrm{s},i} \boldsymbol{Q}_{\mathrm{s},i}^\mathrm{T} \boldsymbol{K}_{\mathrm{s},i}^\diamond \boldsymbol{Q}_{\mathrm{s},i} & \boldsymbol{0} \\ \boldsymbol{0} & \beta_{\mathrm{a},i} \boldsymbol{Q}_{\mathrm{a},i}^\mathrm{T} \boldsymbol{K}_{\mathrm{a},i}^\diamond \boldsymbol{Q}_{\mathrm{a},i} \end{bmatrix}, \tag{11}$$

assuming a Rayleigh damping model for each substructure with the corresponding Rayleigh damping parameters α_s and β_s for the structural domain and β_a for the fluid partition. For fluid-filled pipes, a considerable improvement of the fluid damping model is achieved using an advanced modeling approach including wall friction effects which is the dominant damping mechanism in thin pipes. The advanced fluid damping model is based on a complex wave number and incorporates the frequency dependent wall friction between the acoustic fluid and the pipe shell. A complete derivation of the improved fluid damping model and its integration in the finite element analysis is beyond the scope of this paper. The interested reader is refered to [18, 19]. In frequency domain, Eq. (8) leads to

$$\left(-\boldsymbol{M}_\mathrm{g}\omega^2 + \mathrm{i}\omega\boldsymbol{D}_\mathrm{g} + \boldsymbol{K}_\mathrm{g}\right)\hat{\boldsymbol{q}} = \hat{\boldsymbol{f}}_\mathrm{g}, \tag{12}$$

such that a harmonic analysis is performed using the inverse of the dynamic stiffness matrix as transfer function. The results are expanded to full space in order to obtain the transfer function of interest.

Rubin Method

In contrast to the Craig-Bampton method, the Rubin method is a free-interface method and is applied for the structural domain. Further details can be found in [9].

Applications

Now, two industrial applications are presented, where the different model reduction techniques are applied.

Hydroacoustics of Automotive Piping Systems

The first example is a fluid-filled piping system which is characterized by a heavy fluid-structure coupling between water inside the pipe and the flexible shell. The Craig-Bampton method as explained in Section 2.1 is used as model reduction and substructuring technique to solve the fully coupled system equations. The focus of this section is the hydroacoustic analysis of thin piping systems as found in brake and fuel pipes. The Craig-Bampton method is now applied to a more complex piping system consisting of a curved brake pipe (E = 206 GPa, ρ_S = 7900 kg/m^3, ν = 0.3, lengths 0.7 + 0.3 m) with an outer radius of 3 mm and a wall thickness of 0.7 mm, two steel joints (the so-called clips) and a plate as target structure (E = 180 GPa, ρ_S = 7900 kg/m^3, ν = 0.3, lengths 0.3 x 0.3 x 0.001 m). The pipe is filled with water (c = 1460 m/s, ρ_0 = 1000 kg/m^3). The fluid wave strongly interacts with the flexible pipe shell, which leads to a fluid wave speed of 1408 m/s as opposed to the free sound speed of c = 1460 m/s. This phenomenon is described by Korteweg's equation [22]. The investigated pipe configuration is of practical importance since pressure pulsations in the fluid and strong fluid-structure coupling result in a structural excitation of the brake pipe. The pressure-induced structure-borne sound is transferred to the target structure by the clips as explained in [4]. Fig. 1 shows the pipe configuration assembled by 9 substructures (five straight pipe sections, one elbow, two clips and the plate). The application of the Craig-Bampton method reduces the model order from 55818 DOFs to 2566 DOFs. The additional interface reduction leads to 1118 DOFs. To validate the overall simulation method, the measured and computed hydroacoustic (or hydraulic) transfer function $H_{p1\rightarrow p2}$ is shown in Fig. 1. The measurement is conducted with the same setup as explained before. Again, the correlation between experiment and simulation is very good, both for the obtained hydraulic resonances and the predicted damping in the fluid path. Strong acoustic-structure coupling is observed for a frequency around 1800 Hz, where a hydraulic and a structural resonance coincide. Another fluid-structure coupled mode is visible around 3600 Hz. Note that the observed coupled modes are very sensitive with respect to the structural configuration and the pipe mounting position.

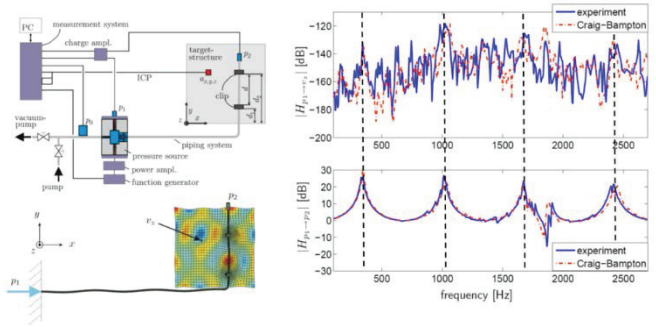

Abbildung 1: Left: Experimental setup of the hydraulic test bench and finite element model of the brake-pipe system with boundary conditions (vibration mode at 1030 Hz). Right: measured and computed hydraulic transfer function |Hp1→p2| and vibro-acoustic transfer function |Hp1→vz|.

Vibro-Acoustic Analysis of an Exhaust System

In this section, pressure-induced vibrations of a production series rear muffler as depicted in Fig. 2 are investigated. Please note, that for simplicity the inner structural parts of the rear muffler are removed. The periodically blown out exhaust gas leads to pressure pulsation within the exhaust system. These pulsations excite structural vibrations, which then additionally contribute to the sound radiation of the system. It is reported that this so-called surface radiated noise might dominate the noise radiated at the orifice [23, 24, 25, 5]. In this work, the focus is set on the pressure-induced vibrations and not on the sound radiation. In order to quantify the pressure-induced vibrations of the rear muffler, the transfer function, $H_{p\rightarrow u}$, between the acoustic pressure at the inlet and the structural deflection at 4 locations on the surface is determined (cf. Fig. 2(b)). The acoustic pressure at the inlet is measured by making use of the two-microphone-method [26]. For the simulation a finite element model is set up with 179808 structural DOFs and 143602 fluid DOFs.

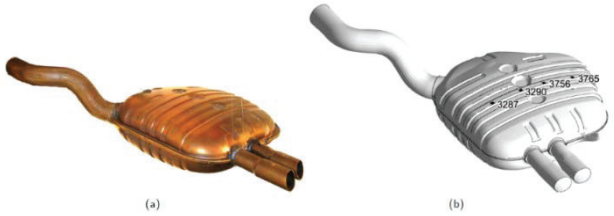

Abbildung 2: (a) Series rear muffler and (b) CAD model.

For an efficient simulation a reduced model is computed using a combined formulation of Craig-Bampton and Rubin method. The Rubin method is applied for the structural domain. The modal damping values obtained from an experimental modal analysis are incorporated in the damping matrix. The Craig-Bampton method is employed for the fluid domain. For each domain, 40 free-interface and fixed-interface normal modes are retained, respectively. The interface DOFs on the inlet and outlets sum up to 444 structural DOFs and 211 fluid DOFs yielding the same number of constraint modes and attachment modes, respectively. It is worth noting, that the interior acoustic fluid intersect with the surrounding fluid at the orifices. Previous investigation showed, that a radiation impedance condition approximates sufficiently accurate the occurring interaction at this cross-section [27]. The impedance condition yields complex entries in the damping matrix D_a [28]. For the frequency sweep computations between 300Hz and 600Hz (with a step step size of 1Hz) the reduced-order models clearly outperform the full-order solution. A speedup of approximately factor 100 is obtained. The plots in Fig. 3 show a comparison between the experimental (solid, black line) and simulative results (dashed, blue line). Each subplot represents the magnitude of the transfer function $H_{p\rightarrow u}$ for one node on the surface of the rear muffler, see Fig 2(b).

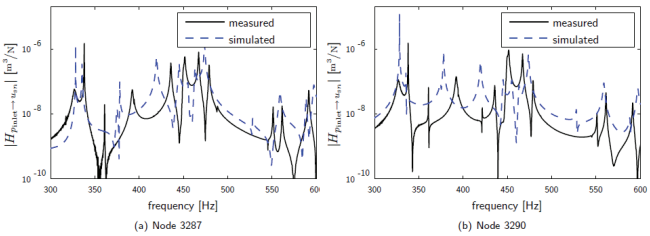

Abbildung 3: Pressure-induced structural vibrations. Comparison of experimental and simulative results.

A strong excitability via the the acoustic path is observed for all points - $H_{p\rightarrow u}$ spans more than four orders of magnitude within the depicted frequency range between 300Hz and 600Hz. A comparison of the eigenfrequencies with the results of an experimental modal analysis reveals that the reasonance

frequencies are reached at eigenfrequencies of the structure. This explains that the surface radiated noise shows a strongly tonal characteristic. All four subplots show a good agreement between experiments and simulations. It is worth noting, that the simulation is capable to predict the transfer function both qualitatively and quantitatively. The proposed method is thus suitable to efficiently predict pressure-induced vibrations in an early development stage and is capable to prevent cost-intensive modifications and time-consuming experiments.

Conclusion

The Craig-Bampton and the Rubin method are successfully applied to fluid-structure coupled systems in order to achieve moderate computation times and computer memory. The hydro- and vibro-acoustic response of two automotive applications is analyzed showing the applicability of the described component mode synthesis. For heavy fluid-structure coupling as in the case of fuel and brake pipes, the fluid and structural partition need to be fully coupled to compute the corresponding component modes and to capture the strong interaction between the fluid and the flexible pipe shell. For light acoustic fluid-structure coupling as in the case of an exhaust system, uncoupled component modes of both the acoustic and structural domain can be used to compute a reduced model. The results of the numerical simulation are compared to dynamic measurements. Good agreement is achieved with respect to hydro- and vibro-acoustic transfer functions of complex fluid-structure coupled systems.

References

[1] M. Maess. Methods for Efficient Acoustic-Structure Simulation of Piping Systems, Dissertation, 2006.

[2] M. Maess, J. Herrmann, L. Gaul. Finite element analysis of guided waves in fluid-filled corrugated pipes. J. of the Acoustical Society of America, 121:1313–1323, 2007.

[3] J. Herrmann, M. Maess, and L. Gaul. Substructuring including interface reduction for the efficient vibro-acoustic simulation of fluid-filled piping systems. MSSP, 24:153–163, 2010.

[4] J. Herrmann, T. Haag, S. Engelke, L. Gaul. Experimental and numerical investigation of the dynamics in spatial fluid-filled piping systems. In Proc. of Acoustics, Paris, 2008.

[5] M. Junge, F. Schube, L. Gaul. Sound Radiation of an Expansion Chamber due to Pressure Induced Structural Vibrations. In Proc. of DAGA, Stuttgart, 2007.

[6] O. Zienkiewicz and R. Taylor. The Finite Element Method. Butterworth-Heinemann, Oxford, 2000.

[7] D. Brunner, M. Junge, and L. Gaul. A comparison of fe-be coupling schemes for large scale problems with fluid-structure interaction. International Journal for Numerical Methods in Engineering, 77:664–688, 2009.

[8] R. R. Craig, M.C.C. Bampton. Coupling of substructures for dynamic analysis. AIAA Journal,6:1313–1319, 1968.

[9] S. Rubin. Improved component-mode representation for structural dynamic analysis. AIAA J.,13:995-1006,1975.

[10] G. C. Everstine. A symmetric potential formulation for fluid-structure interaction. Journal of Sound and Vibration, 79:157–160, 1981.

[11] M. Maess and L. Gaul. Substructuring and model reduction of pipe components interacting with acoustic fluids. MSSP, 20:45-64, 2006.

[12] E. Balmés, A. Bobillot. Iterative technique for eigenvalue solutions of damped structures coupled with fluids. AIAA 43. Structures, Structural Dynamics, and Materials Conference, 168:1–9, 2002.

[13] R. J. Guyan. Reduction of stiffness and mass matrices. AIAA Journal, 3:380, 1965.

[14] J. Herrmann, M.Maess, L. Gaul. Efficient substructuring techniques for the investigation of fluid-filled piping system. Proc. of IMAC XXVII, Orlando, 2009.

[15] M. Junge, D. Brunner, J. Becker, L. Gaul. Interface reduction for the Craig-Bampton and Rubin Method applied to FE-BE coupling with a large fluid-structure interfaces. Int. Journal for Num. Methods in Engineering, 77(12):1731-1752, 2008.

[16] E. Brechlin and L. Gaul. Two methodological improvements for component mode synthesis. In 25. International Seminar on Modal Analysis, Leuven, 2000.

[17] D. Rixen. A dual Craig-Bampton method for dynamic substructuring. Journal of Computational and Applied Mathematics, 168:383–391, 2004.

[18] J. Herrmann, M. Spitznagel, and L. Gaul. Fast FE-analysis and measurement of the hydraulic transfer function of pipes with non-uniform cross section. In Proc. of NAG/DAGA, Netherlands, 2009.

[19] H. Theissen. Die Berücksichtigung instationärer Rohrströmung bei der Simulation hydraulischer Anlagen. Ph.D. thesis, RWTH Aachen, 1983.

[20] R. R. Craig Jr. Coupling of substructures for dynamic analyses: An overview. In Proceedings of the AIAA Dynamics Specialists Conference, Atlanta, GA, 3–6 April 2000. Paper No. 2000-1573.

[21] J. Herrmann, T. Haag, L. Gaul., K. Bendel, H. G. Horst. Experimentelle Untersuchung der Hydroakustik in Kfz-Leitungssystemen. In Proc. of DAGA, Dresden, 2008.

[22] D.J. Korteweg. On the velocity of sound propagation in elastic pipes (in German: Über die Fortpflanzungsgeschwindigkeit des Schalles in elastischen Röhren). Ann. Phys., 5:525–542, 1878.

[23] J.-F. Brand, P. Garcia, and D. Wiemeler. Surface radiated noise of exhaust systems - calculation and optimization with CAE. In Proceedings of the SAE 2004 World Congress & Exhibition, volume 01, 2004.

[24] J.-F. Brand and D. Wiemeler. Surface radiated noise of exhaust systems – structural transmission loss test rig, part 1. In Proceedings of the CFA/DAGA, Strasbourg, 22– 25 March 2004.

[25] J.-F. Brand and D. Wiemeler. Surface radiated noise of exhaust systems – structural transmission loss test rig, part 2. In Proc. of the ISMA, 20–22 September 2004.

[26] A. F. Seybert, D. F. Ross. Experimental determination of acoustic properties using a two-microphone random-excitation technique. Journal of the Acoustical Society of America, 61(5):1362 – 1370, 1977.

[27] H. Levine and J. Schwinger. On the radiation of sound from an unflanged circular pipe. Physical Review, 73(4):383 – 406, 1948.

[28] L. Gaul, D. Brunner, M. Junge. Coupling a fast boundary element method wih a finite element formulation for fluidstructure interaction. In S. Marburg, B. Nolte (eds.), Computational Acoustics of Noise Propagation in Fluids. Springer Berlin Heidelberg, 2008.